A Novel Nonpeptide HIV-1 Protease Inhibitor: Elucidation of the Binding Mode and Its Application in the Design of Related Analogs

Elizabeth A. Lunney,*,† Susan E. Hagen,† John M. Domagala,† Christine Humblet,† Janet Kosinski,† Bradley D. Tait,† Joseph S. Warmus,† Michael Wilson,† Donna Ferguson,† Donald Hupe,† Peter J. Tummino,† Eric T. Baldwin,‡ T. N. Bhat,‡ Beishan Liu,‡ and John W. Erickson‡

Parke-Davis Pharmaceutical Research, Division of Warner Lambert, 2800 Plymouth Road, Ann Arbor, Michigan 48105-2430, and Structural Biochemistry Program, NCI-Frederick Cancer Research and Development Center, PRI/DynCorp, Frederick, Maryland 21702

Received April 28, 1994®

HIV-1 protease has been identified as a significant target enzyme in AIDS research. While numerous peptide-derived inhibitors have been described, the identification of a nonpeptide inhibitor remains an important goal. Using an HIV-1 protease mass screening technique, 4-hydroxy-3-(3-phenoxypropyl)-2*H*-1-benzopyran-2-one (**1**) was identified as a nonpeptide competitive inhibitor of the enzyme. Employing a Monte Carlo-based docking procedure, the coumarin was docked in the active site of the enzyme, revealing a binding mode that was later confirmed by the X-ray crystal analysis. Several analogs were prepared to test the binding interactions and improve the overall binding affinity. The most active compound in the study was 4,7-dihydroxy-3-[4-(2-methoxyphenyl)butyl]-2*H*-1-benzopyran-2-one (**31**).

Introduction

Extensive research to identify a combatant of the human immunodeficiency virus (HIV-1) has targeted the HIV-1 protease enzyme.[1,2] This macromolecule processes HIV polyproteins to produce structural and functional proteins, including the protease itself, and has shown to be essential for viral replication.[3–6]

HIV-1 protease, a member of the aspartic protease family of enzymes,[7,8] is active as a homodimer. Each monomer consists of 99 amino acids and contributes one aspartic acid to the catalytic dyad of the symmetrical enzyme (Figure 1). Multiple X-ray crystal structures have been solved for the HIV-1 protease, both native and complexed, and have been the source of extensive structural and mechanistic information, as well as the subject of recent reviews.[9,10] The enzyme has two antiparallel β-hairpin flaps which cover the ligand in the active site. A conserved water molecule, H_2O301, is situated between the flaps and the peptidomimetic analogs and engages in a hydrogen-bonding network involving the ligand and the amide nitrogens of Ile50/150 in the β-hairpins. Overall, the peptide-like analogs bind to HIV-1 protease in an extended conformation with their amide groups involved in conserved hydrogen bonds with the active site residues and H_2O301 (Figure 2). The peptidomimetic inhibitors generally contain transition state mimetics that bind at the catalytic aspartic acids. Eighteen potential hydrogen bond donors and acceptors exist in the active site,[10] although certain smaller potent inhibitors participate in as few as six or eight.[11,12] The inhibitor side chains occupy subsites that alternate above and below the backbone chain, which are designated according to the convention of Schechter and Berger (P1, P2..., S1, S2...).[13] The P2–P2′ span of the inhibitor has been indicated as the critical region for potent binding.[14]

In recent years, numerous peptide-derived HIV-1 protease inhibitors have been reported, assisted by the concurrent availability of the X-ray crystal structures of protease–inhibitor complexes.[9,10,15,16] However, like the structurally related renin inhibitors, these analogs have properties associated with peptides and, therefore, generally lack the bioavailability requirements essential for cellular and oral activity.[17] Thus while peptide-like analogs with potent inhibitory activity can be designed, limitations exist in their usefulness as therapeutic agents. For this reason, the identification of a low molecular weight, nonpeptide HIV-1 protease inhibitor, while a formidable challenge, has become a focal point in AIDS research. Various methodologies and techniques have been applied in striving toward this goal (Chart 1). Using database searching, the program DOCK[18] screens molecular structures from a 3-dimensional database by fitting them into a binding site represented by overlapping nonconcentric spheres. Through this methodology, haloperidol was identified as a nonpeptide inhibitor lead.[19] In a different variation of database searching, a pharmacophore model was used to search a 3-dimensional database leading to the design of the potent cyclic urea inhibitor, DMP323.[20] This compound contains a diol function that interacts at the catalytic dyad, and, in a unique interaction, the urea

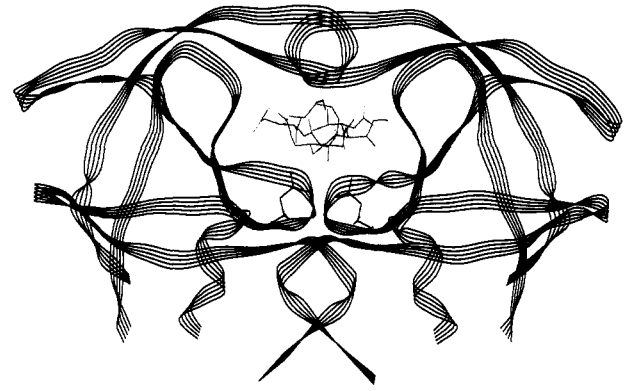

Figure 1. Ribbon backbone trace of the HIV-1 protease from the X-ray crystal complex with the MVT-101 inhibitor[30] (gray). The catalytic Asp25/125 and H_2O301 are shown in black.

† Parke-Davis Pharmaceutical Research.
‡ NCI-Frederick Cancer Research and Development Center.
® Abstract published in *Advance ACS Abstracts*, August 1, 1994.

0022-2623/94/1837-2664$04.50/0

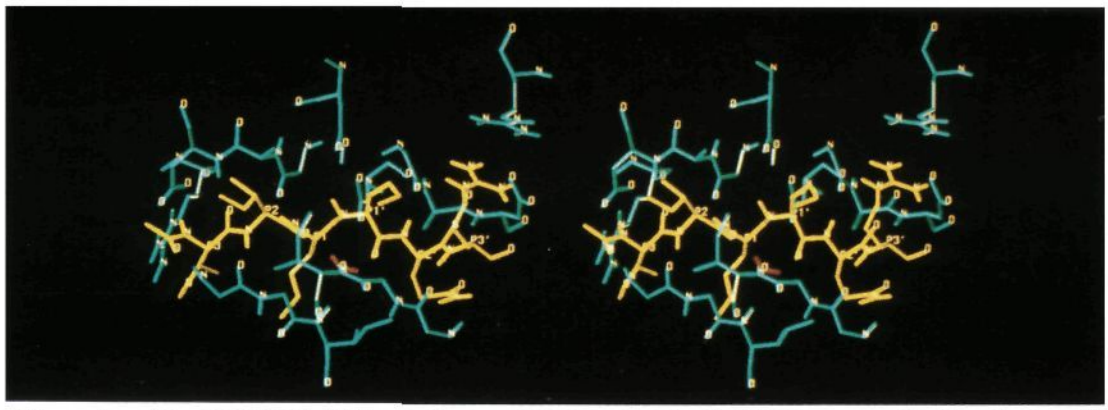

Figure 2. Stereoview of the MVT-101 inhibitor (yellow) and H_2O301 (red) in the HIV-1 protease binding site (cyan).[30]

Chart 1. Nonpeptide HIV-1 Protease Inhibitors

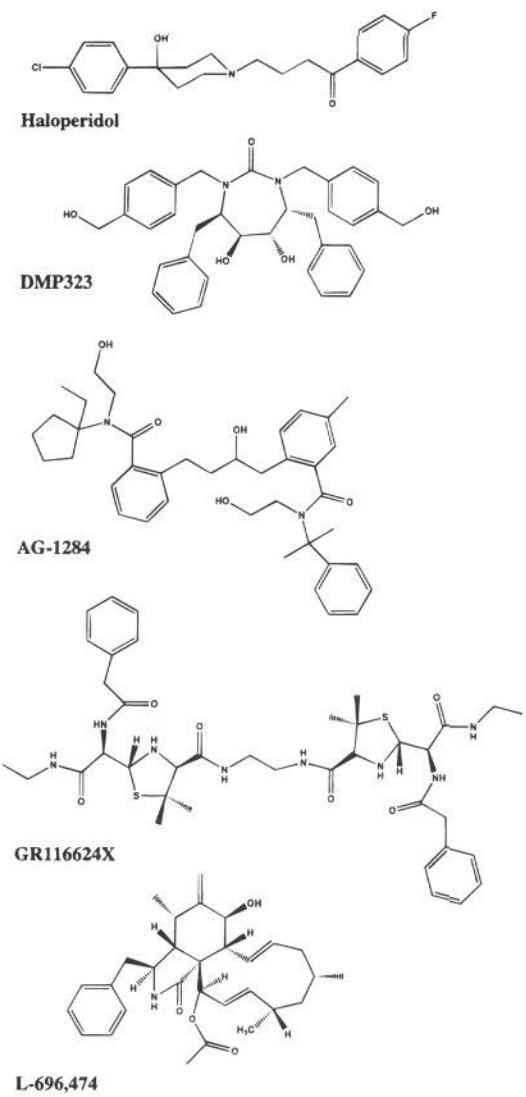

carbonyl displaces H_2O301. In a second general approach, structure-based de novo design was employed in the discovery of AG-1284[21] having overall excellent properties. Alternatively, mass biological screening of compound libraries led to the design of a penicillin-derived dimer, GR116624X, with nanomolar potency.[22] Another screening process involving isolations from fungus fermentations identified a cytochalasin derivative, L-696,474, as an HIV-1 protease inhibitor.[23]

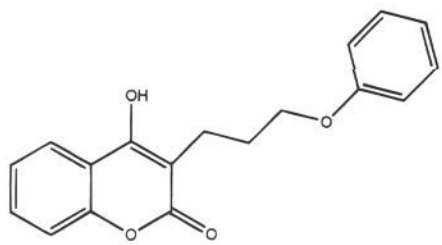

Figure 3. PD099560 (**1**).

In our endeavor to identify a nonpeptide HIV-1 protease inhibitor, we have applied the mass screening technology using our chemical database. A coumarin derivative, PD099560 (Figure 3), has been identified as a low micromolar (μM) competitive inhibitor of HIV-1 protease having a K_i of 1.0 μM.[24] This small molecule contains no amide bonds and no chiral centers. Given these structural features, the competitive inhibition results, and the low K_i, PD099560 was selected as a prototype for chemical and biological study as well as for X-ray determination in the protease enzyme. In the meantime, molecular modeling studies were initiated with the HIV-1 protease crystal structure to predict the bound conformation of the compound. This class of small nonpeptide inhibitors was unprecedented in known HIV-1 protease/inhibitor crystal structures. This further increased the complexity of the docking studies, which now had to address the selection of solvation state and flap orientation, as well as consider the possibility of multiple binding modes. Nonetheless, the modeling studies were carried out and used in the design of novel inhibitors. Subsequently, the X-ray crystal structure of the PD099560 complex was solved and provided valuable information that indeed confirmed the hypotheses generated from the molecular modeling. The new data were also used to refine the modeling and in turn were applied to ligand design. Herein we describe the successful application of compound mass screening to identify a lead structure, followed by a collaborative process involving molecular modeling, protein crystallography, and chemical synthesis, to elaborate the initial "hit" in the design of inhibitors of the targeted HIV-1 protease enzyme.

Results and Discussion

Chemistry. The majority of the coumarins prepared for this study were synthesized as outlined in Scheme 1. Methyl salicylate (**2**) was protected as the 2-(methoxyethoxy)methyl (MEM) ether prior to ester hydrolysis

Scheme 1[a]

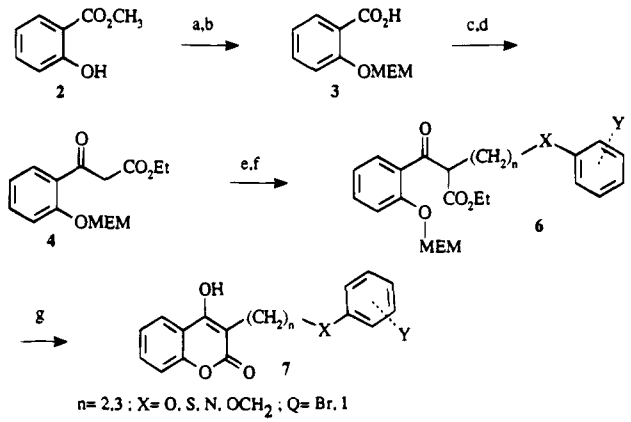

[a] (a) NaH, then MEM chloride; (b) NaOH; (c) CDI; (d) $EtO_2CH_2CO_2K$, $MgCl_2$; (e) NaOEt; (f) Q-$(CH_2)_n$-X-C_6H_4Y (**5**); (g) TFA or $MeSO_3H$.

Table 1. Preparation of Alkylating Agents **5a–m** and Acylating Agents **9a–d**

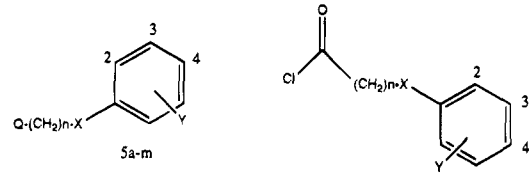

compd	Q	*n*	X	Y	method of prep[a]
5a	Br	3	O	H	comm
5b	Br	3	O	3-Cl	method A
5c	Br	3	O	3-CO_2Et	method A
5d	Br	3	O	3-CN	method A
5e	Br	3	O	3-NO_2	method A
5f	Br	3	O	2-OCH_3	method A
5g	Cl	3	S	H	comm
5h	Br	3	NCH_2Ph	H	ref 44
5i	Br	3	NPh	4-F	ref 44
5j	Br	2	O	H	comm
5k	I	2	OCH_2	H	method B
5l	I	3	OCH_2	H	method B
5m	I	3	O	*c*-hexyl[b]	method C
9a		2	CH_2	H	comm[c]
9b		2	CH_2	4-OCH_3	comm[c]
9c		2	CH_2	2-OCH_3	ref 45[d]
9d		3	O	H	comm[c]

[a] Methods A, B, and C refer to the Experimental Section; comm refers to a chemical which is commercially available. [b] *c*-Hexyl refers to "cyclohexyl"—the phenyl ring in **5** is replaced with a cyclohexyl group. [c] Corresponding acid is commerically available. [d] Corresponding acid is synthesized herein.

under basic conditions. The resulting acid **3** was converted to the imidazolide, which was further elaborated to ketoester **4** via treatment with a mixture of anhydrous magnesium chloride and ethyl potassium malonate. This pivotal intermediate **4** was then deprotonated with sodium ethoxide, and the anion so generated could be quenched with a variety of substituted alkyl halides—ethyl or propyl halides containing a phenoxy, benzyloxy, thiophenyl, or amino moiety in the chain; these alkyl halides were either commercially available or readily prepared as noted in Table 1. Compounds **6** were generally obtained in 60–70% yield after chromatography. Treatment of **6** with trifluoroacetic acid or methanesulfonic acid effectively cleaved the MEM protecting group and promoted the ring closure to the desired benzopyran-2-one **7** all in one step.

An alternative approach to the target compounds is presented in Scheme 2. Benzopyran-2-one **8** was reacted with the requisite acid chloride (Table 1) in pyridine and piperidine[25] to give the carbon-acylated intermediate **10**. Complete reduction of the ketone to the corresponding alkyl derivative **11** was accomplished cleanly and in excellent yield with sodium cyanoborohydride in acetic acid.[26] This acylation/reduction method worked well for those cases where X = CH_2 or OCH_2 in Scheme 2, that is, for those instances where **9** was a 4-phenyl- or 4-phenoxybutyryl chloride. However, the same methodology failed completely when a 3-phenoxypropionyl chloride was used as the acylating agent **9**. In those instances, both benzopyran-2-one **8** and propionic acid were recovered essentially unchanged from the reaction mixture. For this reason, Scheme 2 could not be employed to prepare the 3-(3-phenoxypropyl) analogs of **1** (that is, compounds **23–30**), a shortcoming which necessitated the invention of Scheme 1.

Scheme 2[a]

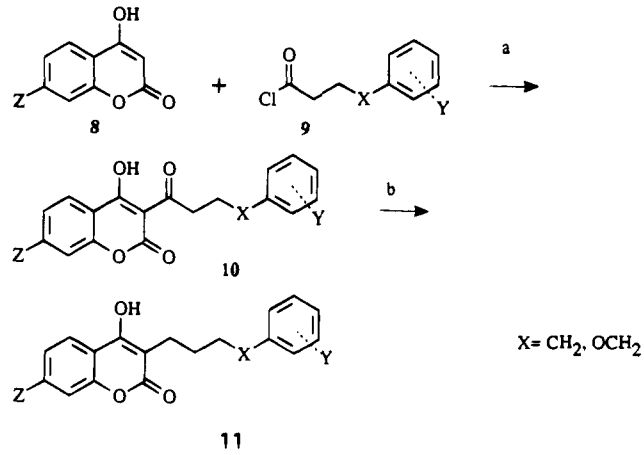

[a] (a) Catalytic piperidine, pyr; (b) $NaCNBH_3$, HOAc.

Molecular Modeling—Docking Studies. As described above, the peptidomimetic inhibitors bind in an extended conformation, and the amide bonds participate in conserved hydrogen bonds with enzyme residues and H_2O301, which is bound to the flaps. In the native enzyme, a water molecule, H_2OCAT, is bound between the catalytic aspartic acid carboxylates. Although not defined in the uncomplexed HIV-1 protease X-ray structure,[15] the water molecule is identified in the crystal structure of native endothiapepsin, a homologous aspartic protease.[27] H_2OCAT is conserved in the various aspartic proteases and postulated to be involved in the nucleophilic attack of the carbonyl group in the amide hydrolysis process.[28] The transition state mimetic groups of the peptide-derived inhibitors displace H_2OCAT upon ligand binding. The conservation in binding revealed by the crystal structures has provided a framework to dock structurally related ligands through the applications of molecular modeling techniques.[14] As the ligand becomes structurally less peptide-like and smaller, the unknowns in predicting its bound conformation increase[21] and numerous questions arise. Would both, one, or neither of the conserved water molecules be displaced by the inhibitor? For the smaller ligands, would multiple binding modes have to be considered and would more than one molecule bind simultaneously at the active site? Would polar interactions replace those conserved with the backbone scaffolding of the peptide ligand? What is the orientation of the flap regions, opened or closed? This latter variable is greatly com-

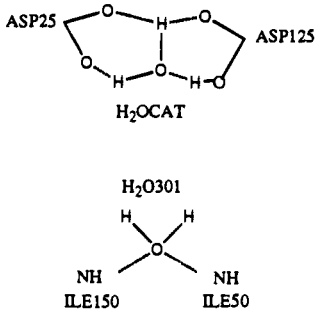

Figure 4. H_2O301 bound at the flap region and H_2OCAT bound at the catalytic dyad.

plicated since the crystal complex with a haloperidol derivative, the first known HIV-1 protease structure with a nonpeptide inhibitor, has an intermediate closure of the flaps.[29]

In the initial molecular modeling studies, the enzyme crystal structure from the HIV-1 protease/MVT-101 complex[30] was used in docking PD099560. The flaps were presented in a closed orientation. This was concluded to be the most reasonable orientation with which to begin, since the enzyme structure should represent the final bound complex and a more tightly held inhibitor would be expected to interact more strongly with the enzyme. This choice was further supported by reports that a more recently solved crystal structure of the complex[29] with the haloperidol derivative exhibited the closed flap conformation. The program Autodock[31] was used to assist in the docking procedure. Starting with the ligand positioned outside the binding region, Autodock randomly maneuvers a ligand with the aim of determining its most favorable bound conformation and orientation in the enzyme or receptor. This is accomplished through using Monte Carlo simulations along rapid energy evaluation, thereby affording an unbiased approach to the process. The procedure was carried out 10 times with three different states of enzyme solvation, i.e., with both (H_2O301 and H_2OCAT), one (H_2O301), or none of conserved water molecules retained in the enzyme binding site (Figure 4). From the 10 simulations with each solvent condition, the binding mode with the lowest interaction energy was evaluated by visual display for favorable contacts in the protease binding site. For the simulations carried out with two water molecules in the active site, the docking result positioned the side chain oxygen and the hydroxyl group within hydrogen-bonding distance of H_2O301 and Gly27(CO), respectively (Figure 5a). No polar interactions were seen with H_2OCAT. The phenoxy ring was situated in the S1 pocket with the coumarin bound in the S2′ site. When only H_2O301 was retained, the docking mode oriented the carbonyl and side chain oxygens so as to interact with H_2O301 and placed the hydroxyl group within hydrogen-bonding distance to Gly127(CO) (Figure 5b). The hydroxyl was 3.4 Å away from Asp129(NH), so a weak interaction could occur. No polar interactions were found with the catalytic dyad. The phenoxy ring side chain was oriented in S1, as was the case for the system where two water molecules were retained; however, the coumarin ring was positioned in the S2 site. The result from the studies where no water molecules were included was the most interesting (Figures 5c and 6). This structure was energy minimized in the binding site, and the interactions were evaluated. The 4-hydroxycoumarin system was positioned to form polar interactions with both the catalytic site and the flap region, thus bridging the width of the cleft. The hydroxyl group was positioned between the carboxylates of the two aspartic acids, within hydrogen-bonding distance to the Asp25 outer oxygen. The ring oxygen formed a hydrogen bond with Ile150(NH), while the carbonyl oxygen was a hydrogen acceptor for Ile50(NH). This latter atom occupied essentially the same position as H_2O301 in the peptidomimetic complexes. The coumarin ring was positioned in the S1 pocket, and the flexible side chain extended through S1′ to the S3′ region with the phenyl pointing in the direction of Arg108. As expected, the bound conformations found in the low-energy results for the three different solvation states varied; however they did begin to define a binding area centered between the S2 and S2′ pockets, the postulated site for potent binding. In the two solvated binding modes, at least two of the key binding pockets proposed to be important for strong affinity with the peptidomimetic analogs were occupied by PD099560. The binding modes also allowed two to four of the polar interactions with the binding site and H_2O301 that are observed with the peptidomimetic analogs. For the unsolvated state, the feasibility of simultaneously displacing H_2OCAT at the catalytic dyad and H_2O301 at the flap region was verified. The

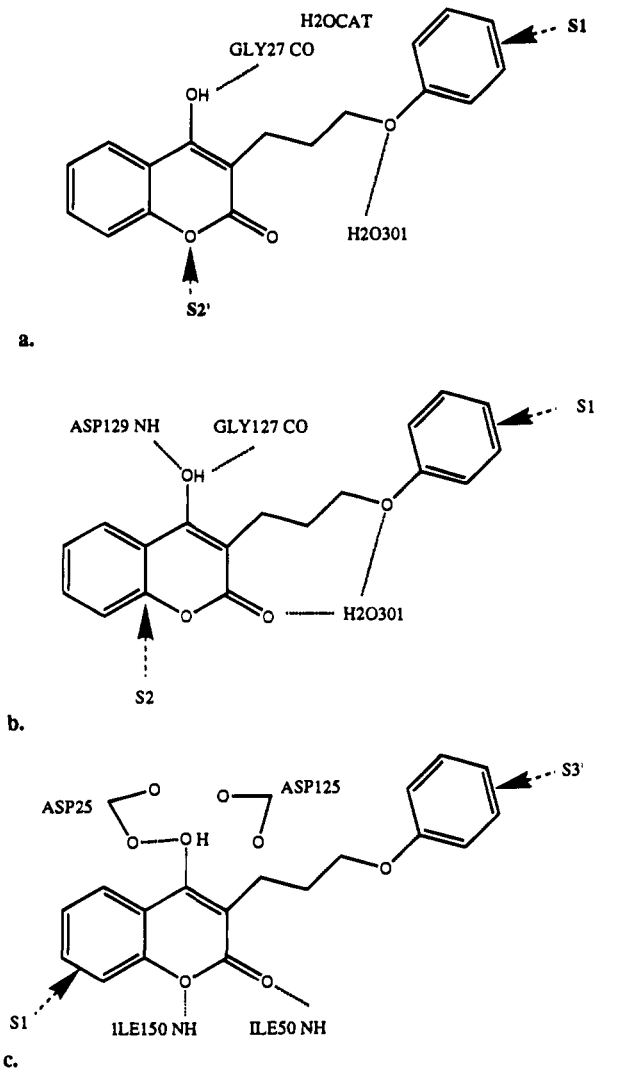

Figure 5. Docking results for PD099560: (a) docking carried out with H_2O301 and H_2OCAT, (b) docking carried out with H_2O301, and (c) docking carried out with no water molecules.

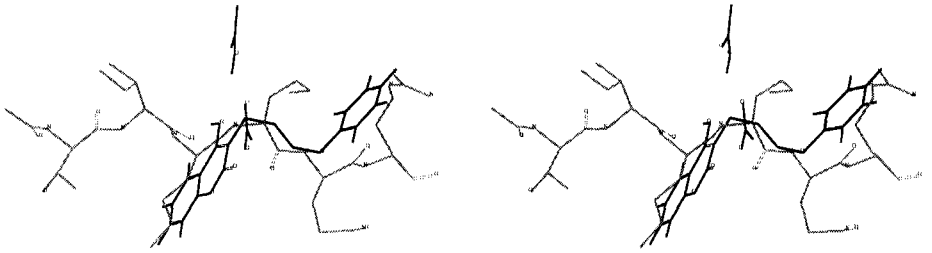

Figure 6. Docking result for PD099560 carried out with no water (black) overlaid with the bound conformation of the MVT-101 inhibitor[30] (gray). The Asp25/125 side chains are also shown.

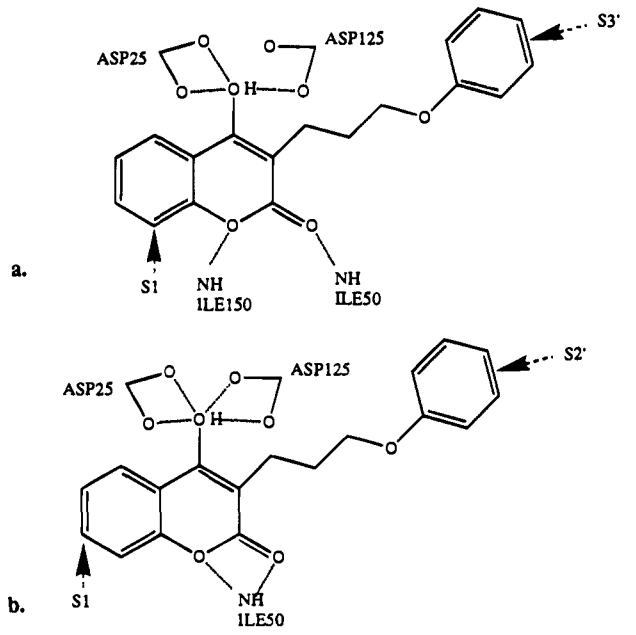

Figure 7. Two binding modes (a and b) for PD099560 in the X-ray crystal structure.

Autodock interaction energies calculated for the three different simulation results that were analyzed differed by less than 2 kcal/mol. Although the interactions overall were significantly reduced relative to the potent peptidomimetic inhibitors, considering the PD099560 structure and micromolar activity, the predicted binding modes were considered reasonable approximations depending on the solvation state and could be applied in the inhibitor design.

X-ray Crystal Structure/Comparison with the Docking Model. The crystal structure of PD099560 complexed with the HIV-1 protease was subsequently solved at 3.0 Å resolution.[32] This structure did indeed show that the 4-hydroxycoumarin ring of the inhibitor displaced both water molecules and presented two bound conformations (Figures 7 and 8). In one binding mode, the hydroxyl group was located between the catalytic aspartates, while both oxygens of the lactone were engaged in hydrogen bonds with the flap region. The fused phenyl ring was oriented in the S1 site, and the flexible side chain extended to the S3′ region toward Arg108. In the second mode of binding, the coumarin ring was oriented more toward the prime binding region such that the lactone oxygens only formed hydrogen bonds with Ile50(NH) in the flap. The hydroxyl group, however, was within hydrogen-bonding range with all the oxygens in the catalytic dyad. The fused phenyl ring of the coumarin system occupied the upper portion of the S1 pocket, while the phenoxy chain originated in the S1′ site and then folded back down to the S2′ region. No water molecules were defined in the structures.

The bound conformation for PD099560 predicted by modeling in the unsolvated system was compared with the first binding mode described for the crystal structure (Figure 9). The binding clefts and inhibitors of both complexes were aligned by performing an rms fit of the α-carbons of the active site residues. In both the modeled and X-ray complexes, the coumarin hydroxyl group was positioned between the catalytic aspartates and each oxygen of the ring lactone interacted with one of the Ile50/150(NH) in the flap loops. With each structure, the flexible side chain adopted a somewhat extended conformation toward S3′ and, in the alignment of the binding sites, a partial overlap of the phenoxy rings was realized. The modeled coumarin ring was oriented at an angle approximately 22° relative to the crystal structure ring, which resulted in the binding of its coumarin phenyl more deeply in the S1 pocket. Overall, the modeling studies proved successful in predicting the first binding mode for PD099560.

Molecular Modeling Studies with the PD099560 X-ray Complex. To assist in inhibitor design, the program GRID[33] was applied to the HIV-1 protease structure from the PD099560 complex with the first binding mode in the absence of the inhibitor. The GRID methodology employs probes to determine favorable interaction sites on the surface of a molecule. Both a water and a methyl probe were used to map key hydrogen-bonding and van der Waals (vdW) interaction sites, respectively (Figure 10). The water probe, contoured at −5 kcal/mol, mapped polar interaction sites that included a large area bordering the catalytic aspartic acids and the approximate location of H_2O301 found in the peptidomimetic complexes. The water probe produced contrasting maps between Gly48 in the flap region and the Asp29-Asp30 sequence (prime side) and between the analogous residues Gly148 and Asp129-Asp130 ("P" side). In the former case, a larger binding contour was determined. Interesting, the methyl probe produced a completely filled contour at −2 kcal/mol on the prime side, while the "P" area represented more of a doughnut shape, indicating the center of this region had reduced van der Waals contact. Upon further inspection of the protein structure, it was noted that the Asp30 side chain was oriented more toward the binding site than the Asp130 on the "P" side. This could account at least in part for the more extensive polar binding region and fuller vdW contour mapped in the prime area. However, beyond this, in comparing the span across these regions, measured by the distance between the α-carbons of Gly49/149 and Ala28/128, the "P" side Gly149−Ala128 distance was 0.73 Å longer than the corresponding prime distance. Therefore the en-

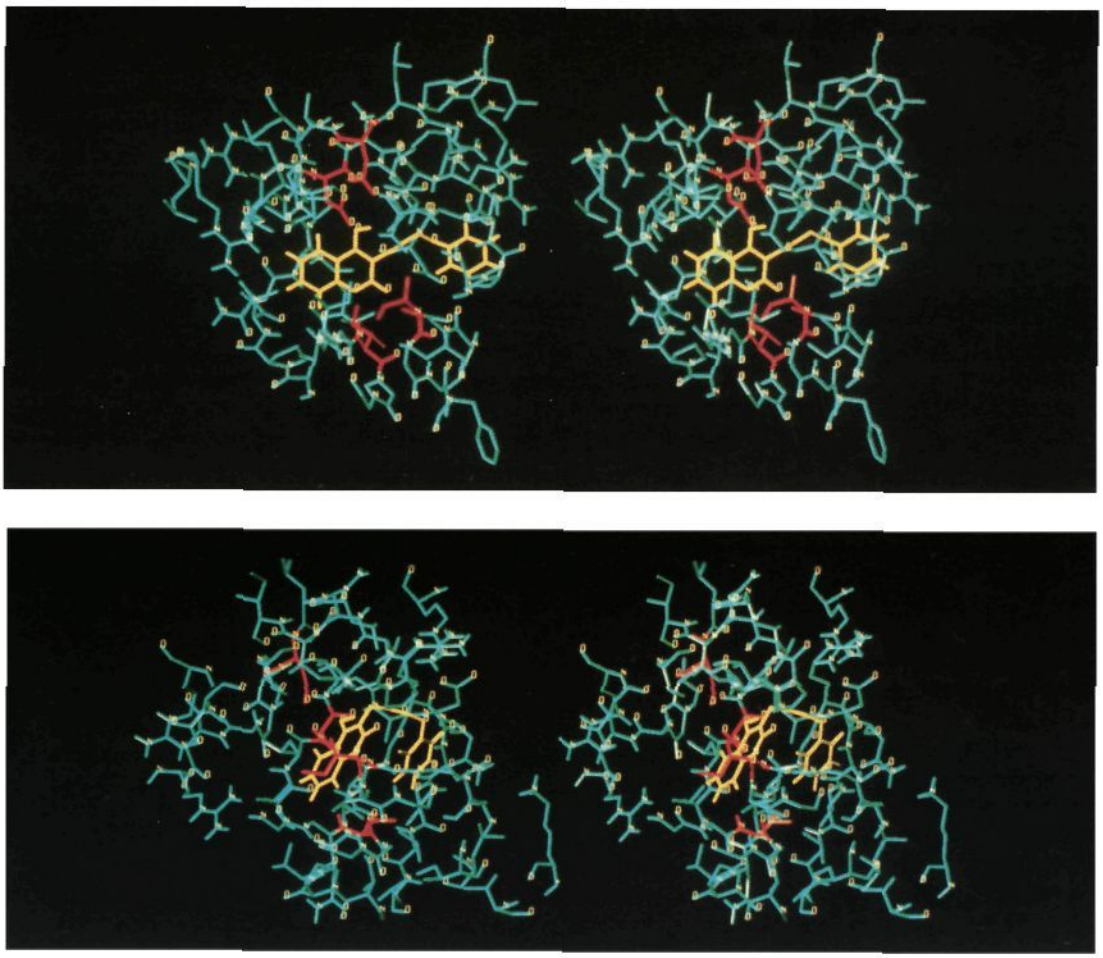

Figure 8. (top) Stereoview of the first binding mode of PD099560 (yellow) in the HIV-1 protease binding site (cyan, with Asp25/125 and Ile50/150 shown in red) extracted from the X-ray crystal structure. (bottom) Stereoview of the second binding mode of PD099560 (yellow) in the HIV-1 protease binding site (cyan, with Asp25/125 and Ile50/150 shown in red) extracted from the X-ray crystal structure.

zyme residues may be too remote from the center of the former site to interact as favorably with a ligand and resulted in the contrasting subsite contours for both the water and methyl probes. Thus, GRID mapped the favorable interaction sites as well as highlighted interaction site differences between the "P" and prime sides. These results can be applied to inhibitor design, especially in the more refined modifications needed to achieve potent analogs.

Inhibitor Design. The analysis of the PD099560/protease crystal complex indicated that the phenoxy oxygen was not involved in any direct polar interaction with the enzyme. To investigate the importance of the oxygen and its location in the side chain, various analogs were synthesized (Table 2). Simple replacement of the oxygen with either carbon or sulfur (**12** and **13**) attenuated the potency by 50- and 10-fold, respectively, with the sulfur analog still providing some favorable interactions. It was evident that the presence of the oxygen was important for binding, but what was its optimal position? The impact of the location of the oxygen was explored. In one series, the side chain length was held constant at four atoms and the oxygen was positioned at a different site in the chain or as a methoxy substituent on the phenyl ring (**16**–**18**). Interestingly, moving the oxygen one position closer to the coumarin ring in **16** or moving the oxygen to the ortho position on the phenyl ring in **18** caused essentially no change in potency relative to the parent. Clearly, some latitude existed in the ideal placement of the oxygen within this region. To test this premise, the methoxy group was substituted in the more remote para position resulting in **17**. As expected, more than a 40-fold decrease in potency was observed, comparable to that seen with the methylene analog **12**. Furthermore, this range in activity indicated that electron donation into the side chain phenyl ring was not of itself important, since **17** and **18** would be expected to have almost identical electron density in the ring system. In another series, the length of the side chain was either decreased (**19**) or increased (**20** and **21**) by one atom. With **21**, the position of the oxygen relative to the coumarin ring as exists in PD099560 was retained but a carbon was inserted between the oxygen and the phenyl ring. Moving both the oxygen and the phenyl closer toward the nucleus (**19**) resulted in a 20-fold drop in potency. This would appear to be due to the change in position of the phenyl group, since the analogous oxygen positioning in **16** did not impact activity. This was further substantiated by **21**, which was essentially equipotent to **19** and positioned only the phenyl ring differently relative to the parent. Going one step further with **20**, in which both the oxygen and the phenyl group are located farther out in the side chain, the activity

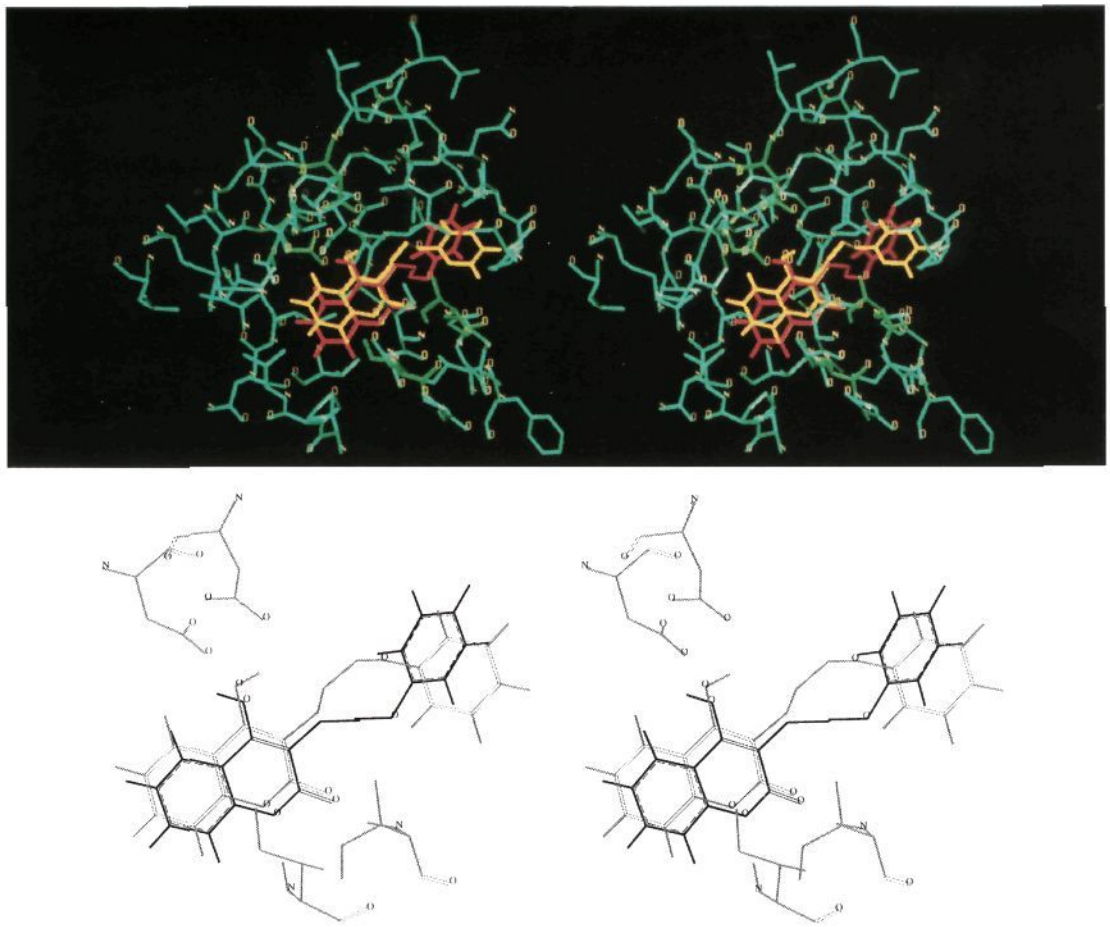

Figure 9. (top) Stereoview of PD099560 from the first binding mode in the X-ray crystal structure (yellow) overlaid with the docking result carried out with no water molecules (red) in the binding site of the PD099560/protease complex (cyan, with Asp25/125 and Ile50/150 highlighted in green). (bottom) Stereoview of PD099560 from the first binding mode in the X-ray crystal structure (gray) overlaid with the docking result carried out with no water molecules (black). Asp25/125 and Ile50/150 from the PD099560/protease complex are also shown.

dropped more dramatically (over 40-fold). To summarize, the position of the oxygen could vary within a certain region and activity could be maintained; however, moving the phenyl group attenuated the potency. Even more detrimental was the concerted displacement of both the oxygen and the phenyl ring away from the coumarin system.

It was surprising that the analysis of the PD099560 crystal complex showed no direct polar interaction of the oxygen with the enzyme structure in either of the determined binding modes for the inhibitor, and yet the structure–activity relationship significantly depended on the oxygen. The resolution of the crystal complex was not refined enough to locate water molecules, so the presence of a water bridge between the ligand and the protein remained a possibility. This phenomenon was observed in the crystal complex of the peptidomimetic inhibitor Ro-31-8959, wherein the C-terminal *tert*-butyl amide binds through ordered water molecules to Asp29(NH) and Gly27(CO).[10] Applying the GRID methodology with the crystal complex for PD099560 in both binding modes, the likelihood of the water-bridged interaction was studied. The inhibitors were included as part of the target molecule in the probe calculations to identify favorable binding sites for water in the entire complex. Water molecules were then manually oriented in the structure. As can be seen from Figure 11 (top) for the extended binding mode, a low-energy binding site for water existed between the phenoxy oxygen and Asp29(NH). For the folded bound conformation, a binding site was determined in which water could form a bridge among the phenoxy oxygen and both the NH and carbonyl of Gly48 in the flap region (Figure 11, bottom). Thus, although a direct interaction was not made between the phenoxy oxygen and the protease in either binding mode, an intervening water molecule could serve as a favorable hydrogen-bonding bridge in both cases. Therefore, the importance of the oxygen might very well be linked to its ability to be an acceptor in the water interaction. This explanation was further supported by the relative potency observed for **13** containing the sulfur replacement, which can also act as a hydrogen bond acceptor. As is seen in Table 2, **13** is 4-fold more potent than the aliphatic derivative **12**.

One reason for the importance of the phenyl position could be linked to the interaction observed between this group and Arg108 in the first binding mode in the crystal complex (Figure 8, top). Changing the length of the side chain would alter the apparent optimal contact. Compounds **34** and **35** (Table 3) were synthesized to further investigate the importance of this interaction, with **34** allowing a direct comparison to be made between the aromatic phenyl ring versus the cycloalkyl group. In both cases, the potencies were attenuated and thus indicated the loss of a favorable polar interaction between the Arg108 guanidinium

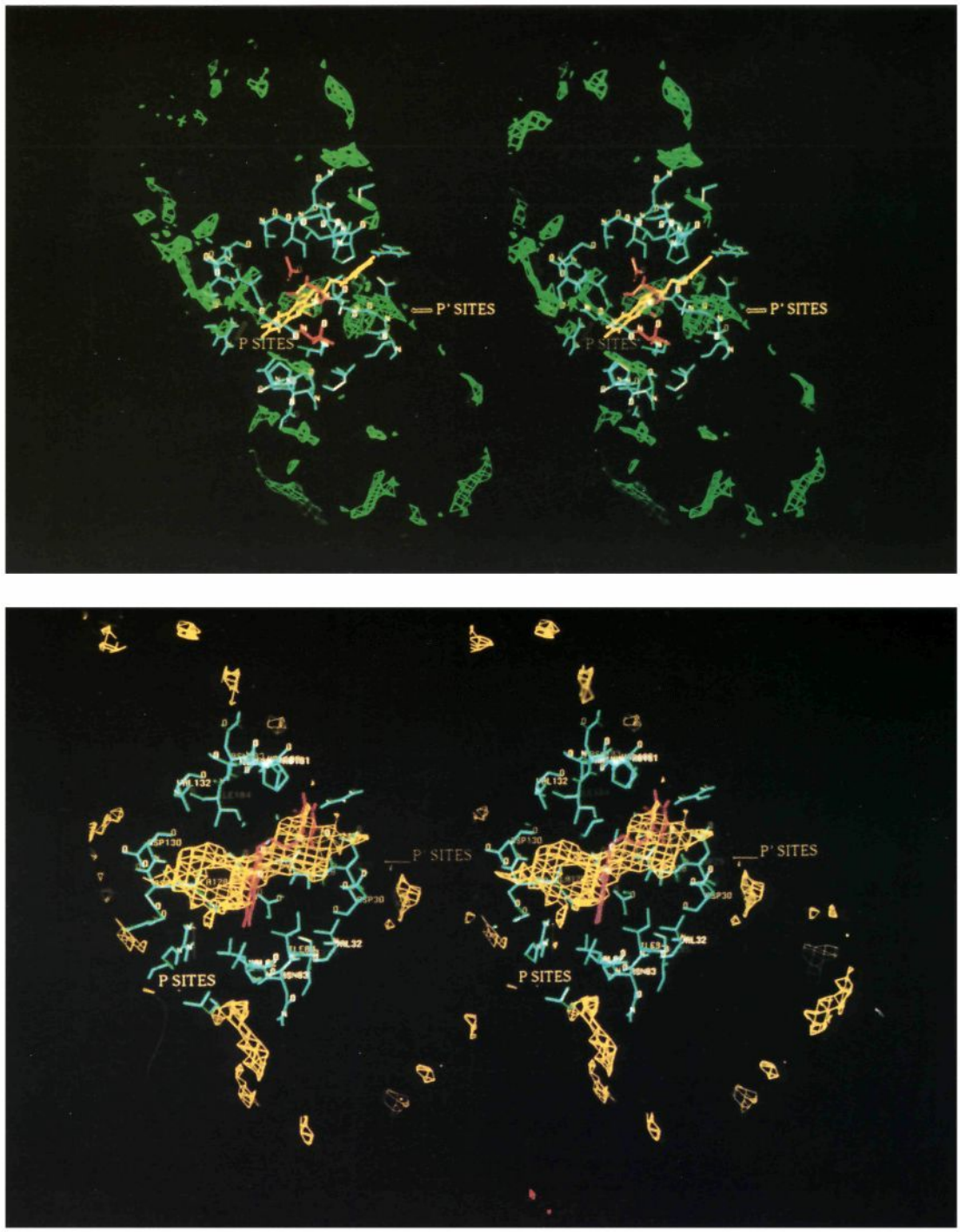

Figure 10. (top) Stereoview of the contour (green) at −5 kcal/mol for the GRID calculations carried out for the enzyme structure (cleft residues in cyan and red) from the HIV-1 protease/PD099560 complex with the first binding mode using a water probe. The inhibitor (yellow) is shown as a point of reference. (bottom) Stereoview of the contour (yellow) at −2 kcal/mol for the GRID calculations carried out for the enzyme structure (cleft residues in cyan) from the HIV-1 protease/PD099560 complex with the first binding mode using a methyl probe. The inhibitor (red) is shown as a point of reference.

group and the phenyl ring. In considering the second binding mode of PD099560, the bulkiness of the cyclohexyl ring relative to a phenyl group could lessen the flexibility of the side chain and its ability to fold back on itself, as is the conformation observed with the phenoxy side chain in the crystal complex.

Substituting a methoxy group at the ortho position of the PD099560 phenoxy ring (**22**, Table 2) reduced the potency (20-fold). Thus the presence of both oxygens in the side chain was not beneficial to binding. The proximity of these oxygens in **22** could result in a strongly bound water molecule in solution, and therefore the desolvation barrier may account for the drop in activity.

A series of compounds in which the meta position of the phenoxy ring was substituted with various groups were designed to pick up favorable interactions with the Arg108 side chain or Gly48(CO) (**23**−**30**, Table 2). These substitutions did not significantly impact the activity, although the nitrile derivative (**29**) was slightly

Table 2. Physical Properties and Inhibitory Activity of Hydroxycoumarins

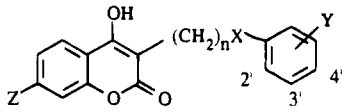

compd	n	X	Y	Z	method of prep[a]	start mater from Table 1	method of purification of final product[b]	yield[c] (%)	mp (°C)	analysis formula (elements analyzed)	IC_{50}[d] (μM)
1	3	O	H	H	D	**5a**	trit, hex:EtOAc	37	124–126	$C_{18}H_{16}O_4$ (C,H)	2.3
12	3	CH_2	H	H	E	**9a**	washed with H_2O	43	160–161	$C_{19}H_{18}O_3$ (C,H)	110
13	3	S	H	H	D	**5g**	trit, hex:EtOAc	35	156–157	$C_{18}H_{16}O_3S{\cdot}0.3H_2O$ (C,H)	26
14	3	NPh	4'-F	H	D	**5i**	chrom	53	143–145	$C_{24}H_{20}FNO_3{\cdot}0.3H_2O$ (C,H,N)	5.5
15	3	NCH_2Ph	H	H	D	**5h**	chrom	27	63–65	$C_{25}H_{23}NO_3{\cdot}0.3H_2O$ (C,H,N)	13
16	2	OCH_2	H	H	D	**5k**	chrom	51	oil	$C_{18}H_{16}O_4{\cdot}0.5H_2O$ (C,H)	4
17	3	CH_2	4'-OCH_3	H	E	**9b**	washed with H_2O	56	129–130	$C_{20}H_{20}O_4$ (C,H)	>100
18	3	CH_2	2'-OCH_3	H	E	**9c**	recrys, EtOH:H_2O	23	123–124	$C_{20}H_{20}O_4{\cdot}0.15H_2O$ (C,H)	1.7
19	2	O	H	H	D	**5j**	washed with hex	43	157–159	$C_{17}H_{14}O_4{\cdot}0.3H_2O$ (C,H)	53
20	4	O	H	H	E	**9d**	washed with H_2O	47	180–181	$C_{19}H_{18}O_4$ (C,H)	>100
21	3	OCH_2	H	H	D	**5l**	trit, hex:EtOAc	38	86–87	$C_{19}H_{18}O_4{\cdot}0.2CH_3SO_3H{\cdot}H_2O$ (C,H)[e]	38
22	3	O	2'-OCH_3	H	D	**5f**	chrom	43	119–120	$C_{19}H_{18}O_5$ (C,H)	44
23	3	O	3'-NO_2	H	D	**5e**	none	44	175–177	$C_{18}H_{15}NO_6{\cdot}0.4CH_3SO_3H{\cdot}2H_2O$ (C,H,N)[e]	4.0
24	3	O	3'-NH_2	H			chrom	45[f]	161–162	$C_{18}H_{17}NO_4{\cdot}0.25H_2O$ (C,H,N)	6.4
25	3	O	3'-CO_2Et	H	D	**5c**	trit, hex:EtOAc	58	125–126	$C_{21}H_{20}O_6{\cdot}0.2H_2O$ (C,H)	1.4
26	3	O	3'-CO_2H	H			none	85[g]	242–244	$C_{19}H_{16}O_6{\cdot}0.3H_2O$ (C,H)	7.0
27	3	O	3'-CH_2OH	H			chrom	52[g]	119–121	$C_{19}H_{18}O_5{\cdot}0.3H_2O$ (C,H)	2.3
28	3	O	3'-Cl	H	D	**5b**	trit, hex:EtOAc	35	169–171	$C_{18}H_{15}ClO_4{\cdot}0.2H_2O$ (C,H)	1.4
29	3	O	3'-CN	H	D	**5d**	none	48	174–176	$C_{19}H_{15}NO_4{\cdot}0.4H_2O$ (C,H,N)	0.67
30	3	O	3'-$CONH_2$	H			washed with H_2O	70[h]	197–198	$C_{19}H_{17}NO_5{\cdot}1.2HCl$ (C,H,N,Cl)	3.9
31	3	CH_2	2'-OCH_3	OH	E	**9b**	recrys, EtOH:H_2O	11	161–162	$C_{20}H_{20}O_5$ (C,H)	0.52
32	3	CH_2	2'-OCH_3	OCH_2Ph	E	**9b**	recrys, EtOH	24	161–162	$C_{27}H_{26}O_5$ (C,H)	>100
33	3	CH_2	2'-OCH_3	OCH_3	E	**9b**	recrys, EtOH:H_2O	28	153–154	$C_{21}H_{22}O_5{\cdot}0.2H_2O$ (C,H)	3.3

[a] Letters refer to the general methods in the Experimental Section; when no letter is present, the method of preparation is included in the Experimental Section in its entirety. [b] Trituration (trit) refers to grinding of the solids under solvent to produce a fine powder. [c] Yield is calculated starting from compound **4**. [d] See experimental. [e] Presence and amount of CH_3SO_3H verified by NMR. [f] Yield from compound **23**. [g] Yield from compound **25**. [h] Yield from compound **29**.

more potent than the parent. The flexibility of the side chain even upon binding, as was evident by the dual binding modes found in the crystal complex, may readily explain the flat structure–activity relationship.

Several side chain derivatives of intermediate activity were prepared and are included in Table 3 (compounds **36**–**38**). Ketone **36** and oxime **37**, both of which contain an oxygen functionality in the chain, displayed a decreased potency relative to the parent **1**. Substitution of a sulfur atom in the side chain adjacent to the coumarin nucleus (compound **38**) also affected the activity deleteriously, although to a lesser extent. Again, given the flexibility of the side chain and the duality of the binding modes, it is not surprising that a variety of C-3-substituted analogs would show moderate efficacy.

Keeping the side chain constant as in **18**, the coumarin ring was substituted at position 7 (**31**–**33**, Table 2). The hydroxyl analog, **31**, emerged as the most potent inhibitor in the entire series at 4-fold the potency of PD099560. Again, an analysis of the crystal complex indicated no direct polar interaction with the enzyme in either conformation. The GRID contour for the crystal complex with the folded inhibitor conformation did however identify a potential binding position for a water molecule that could bridge an interaction between the hydroxyl substitution at position 7 of PD099560 and Gly148(CO) (Figure 12).

One of the first modifications that was pursued involved replacing the coumarin lactone group with a lactam functionality as seen in **39**. As is shown in Table 3, the compound was inactive. This is not surprising upon evaluating both PD099560 binding modes in the protease. In each case, the ring oxygen is a hydrogen acceptor with one of the flap Ile(NH). Substituting the oxygen with the NH would cause repulsion. The inactivity of the lactam derivative did however verify that the small molecule could not adopt a favorable binding mode different from that of the parent compound.

Attempts were made to fill multiple binding sites simultaneously with lipophilic groups and take advantage of the dual side chain binding modes observed in the crystal complex and the favorable van der Waals interaction site predicted by GRID (Figure 10b). The use of N,N-disubstituted side chains, as in **14** and **15**, afforded the introduction of a branched group without the creation of a chiral center. Compound **15** resulted in a 6-fold drop in activity; however the potency of **14** only dropped by a factor of 2. Therefore the basic concept of branching proved feasible, with the lower affinity possibly due to the removal of the favorable oxygen.

While modifying PD099560 to expand to multiple prime binding sites appeared to offer some promise, this was less the case for occupying the S2 pocket left vacant in the PD099560 complex. Unfortunately, the rigid coumarin ring in both binding modes is not well-positioned for substituting groups that could easily probe this site and increase the favorable interactions with the enzyme. Substitutions of the coumarin ring that were made, beyond that described previously, were expectedly uneventful (data not shown).

Conclusion

An HIV-1 protease nonpeptide inhibitor, PD099560, was identified through the mass screening of our

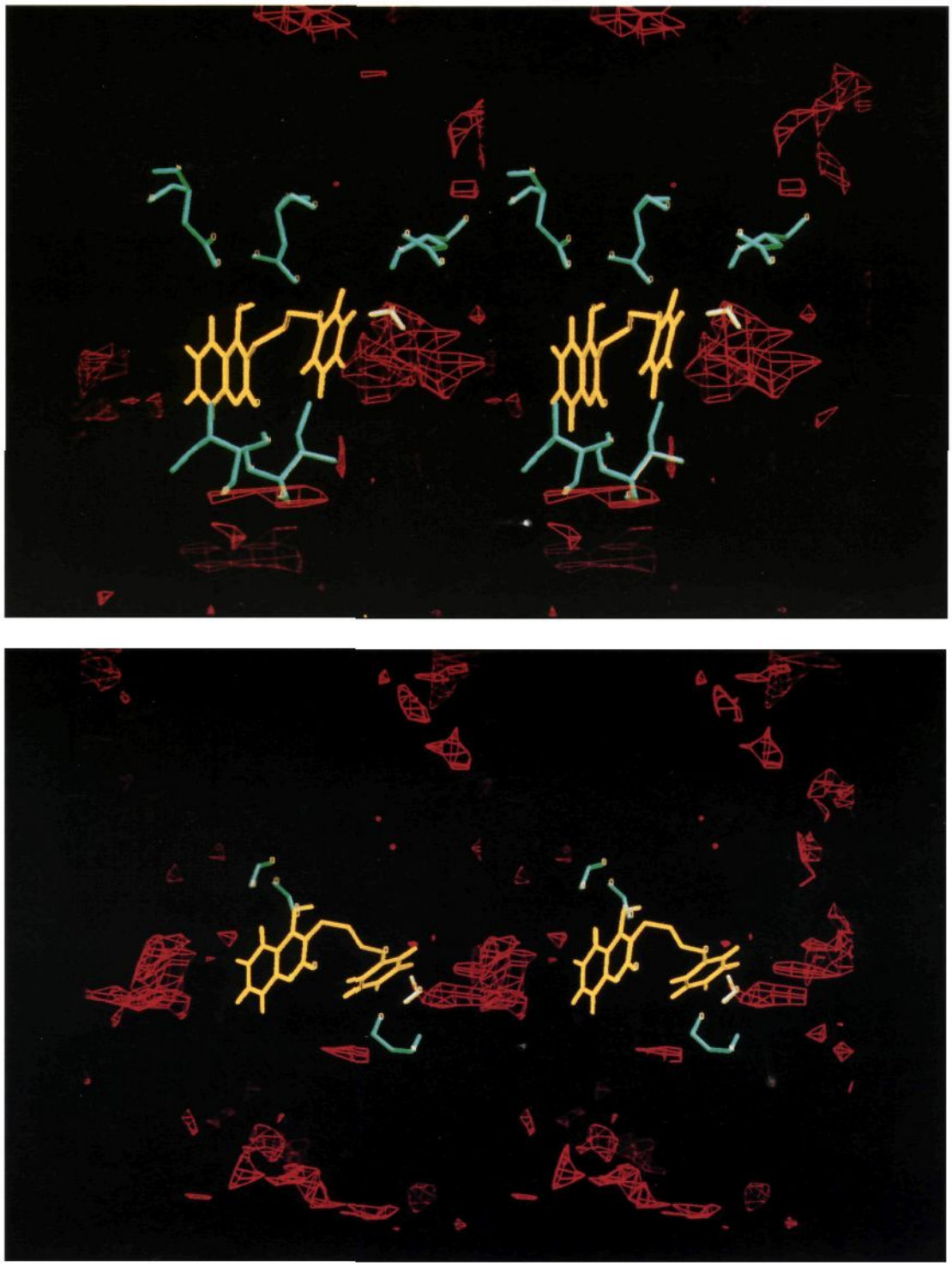

Figure 11. (top) Stereoview of the contour (red) at −5 kcal/mol for the GRID calculations carried out for the HIV-1 protease/PD099560 complex with the first binding mode using a water probe. The inhibitor (yellow), the inserted water (white), and the Asp25/125, Ile50/150, and Asp29 residues (cyan) are also shown. (bottom) Stereoview of the contour (red) at −5 kcal/mol for the GRID calculations carried out for the HIV-1 protease/PD099560 complex with the second binding mode using a water probe. The inhibitor (yellow), the inserted water (white), the Asp25/125 carboxyl groups, and Gly48 (cyan) are also shown.

extensive compound collection. A collaborative process involving modeling, X-ray crystallography, and chemical synthesis was applied in the successful design of novel inhibitors based on the initial "hit". The X-ray structure of the PD099560 complex showed two bound conformations for the inhibitor. The original prediction of the bound conformation of PD099560 using molecular modeling was confirmed by one of the binding modes observed in the X-ray. Although the activity of PD099560 was improved, its modes of binding were not optimal for extending the structure and gaining favorable binding interactions with the enzyme. Replacing the coumarin nucleus with a pyrone system, which lacks the rigid, fused β-phenyl ring, appears to alleviate this problem. Work ongoing with this series will be reported elsewhere.[34]

Table 3. Physical Properties and Inhibitory Activity of Some Miscellaneous 4-Hydroxycoumarins

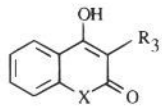

compd	X	R_3	method of prep[a]	start mater from Table 1	method of purification of final product[b]	yield[c] (%)	mp (°C)	analysis formula (elements analyzed)	IC_{50}[d] (μM)
34	O	$CH_2CH_2CH_2O$(*c*-hexyl)	D	**5m**	chrom	20	54−56	$C_{18}H_{22}O_4 \cdot 1.0H_2O$ (C,H)	32
35	O	$CH_2CH_2CH_2OH$			trit, ether	95[e]	109−110	$C_{12}H_{12}O_4 \cdot 1.1H_2O$ (C,H)	86
36	O	$CH_2CH_2C(=O)Ph$	ref 40		recrys, EtOH	68	149−151	$C_{18}H_{14}O_4$ (C,H)	90
37	O	$CH_2CH_2C(=NOH)Ph$			recrys, EtOAC:hex	75[f]		$C_{18}H_{15}NO_4 \cdot 0.5H_2O$ (C,H,N)	71
38	O	SCH_2CH_2OPh	ref 41		chrom	67	120−121	$C_{17}H_{14}O_4S \cdot 0.45H_2O$ (C,H)	24
39	N	$CH_2CH_2CH_2OPh$			trit, ether	4	170−171	$C_{18}H_{17}NO_3$ (C,H,N)	>200

[a] Letters refer to the general methods in the Experimental Section; when no letter is present, the method of preparation is included in the Experimental Section in its entirety. [b] Trituration (trit) refers to grinding of the solids under solvent to produce a fine powder. [c] Unless otherwise noted, the yield is calculated from either compound **4** (Scheme 1) or compound **8** (Scheme 2). [d] See Experimental. [e] Yield from **21**. [f] Yield from **36**.

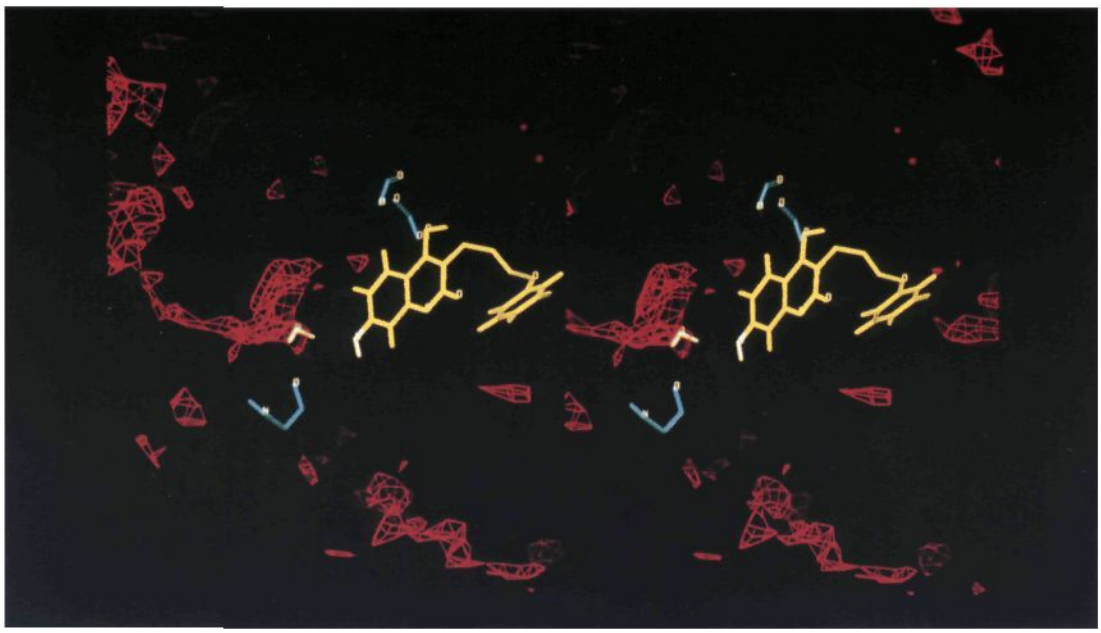

Figure 12. Stereoview of the contour (red) at −5 kcal/mol for the GRID calculations carried out for the HIV-1 protease/PD099560 complex with the second binding mode using a water probe. PD099560 (yellow) substituted at position 7 with a hydroxyl group (white), the inserted water (white), the Asp25/125 carboxyl groups, and Gly148 (cyan) are also shown.

Experimental Section

Protein Inhibition Assay. For determination of IC_{50} values, HIV-1 protease, 6.0 nM final, was added to a solution containing inhibitor, 40 μM substrate III (the undecapeptide H-His-Lys-Ala-Arg-Val-Leu-(*p*-NO_2)Phe-Glu-Ala-norleucine-Ser-NH_2, >97% purity, purchased from Bachem Bioscience, Inc., Philadelphia, PA), and 1.0% DMSO in assay buffer: 1.0 mM dithiothreitol, 0.1% poly(ethylene glycol) (MW 8000), 80 mM NaOAc, 160 mM NaCl, 1.0 mM EDTA, pH 4.7, at 37 °C (total volume, 100 μL). Poly(ethylene glycol) was used in the assay in place of glycerol since the former was reported to be a more effective stabilizing agent of the protease.[35] The final inhibitor concentrations used were 0, (0.1 and 0.2 in some experiments) 0.5, 1, 2, 5, 10, 20, 50, and 100 μM. The solution was mixed and incubated for 5 min and the reaction quenched by addition of trifluoroacetic acid, 2% final. The Leu-*p*-nitro-Phe bond of the substrate was cleaved by the enzyme, and the substrate and products were separated by reversed-phase HPLC. Absorbance was measured at 220 nm, peak areas were determined, and percent conversion to product was used to calculate % control ([% conversion (+ inhibitor)/% conversion (− inhibitor)] × 100).

Molecular Modeling. The molecular modeling was carried out on a 4D/TG35 Silicon Graphics computer using the Sybyl molecular modeling software.[36] PD099560 was docked in the active site of the HIV-1 protease crystal structure using the Autodock program.[31] The protein and H_2O301 coordinates from the HIV-1/MVT-101 complex were used.[30] The inner carboxylate oxygen of one of the catalytic aspartic acids was protonated. The catalytic water was extracted from the native endothiapepsin structure after an rms fit of the aspartic acid carboxylates[27] of the two enzymes. Three affinity grids were calculated for the enzyme with different solvation states, i.e., having both (H_2O301 and H_2OCAT), one (H_2O301), or none of the conserved waters included. Ten simulations with each of the grids were carried out with PD099560 initially oriented outside the binding region. The dielectric was set at 40 to represent overall a partially solvated state. A simulation consisted of 50 cycles, each of which was carried out at constant temperature and contained a multitude of steps. At every step, a displacement occurred in each degree of freedom: translational, rotational, and torsional (six molecular bonds were rotated). An evaluation was then made of the interaction energy with the affinity grid. If the energy dropped, the move was accepted; if the energy rose, the move might be accepted on the basis of Boltzmann distribution. At the end of the cycle, the temperature was reduced and a new cycle was initiated using the conformer with the lowest interaction energy from the previous series of steps. The final structure from each of the 10 simulations was saved with a calculated interaction

energy. Optimizations were performed using the Tripos force field,[36] aggregating the cleft region and the coumarin hydroxyl oxygen and without electrostatics. Hydrogen bonds (XH···Y) were identified by distances between the heavy atoms (X−Y cutoff, ≤3.3 Å) and the XH···Y angle (>90°). In comparing the modeled inhibitor structure with the X-ray, an rms fit of the α-carbons of the cleft residues in the structure containing the model (cleft is defined as residues within 8 Å of the ligand) to the corresponding α-carbons of the X-ray cleft residues was performed. The angle between the coumarin ring in the modeled structure and that in the X-ray was approximated by measuring the angle formed by the position 8a carbon in the modeled coumarin and the carbons at positions 3 and 8a in the X-ray coumarin. The GRID[33] calculations were carried out with a water and a methyl probe and contoured at −5 and −2 kcal/mol, respectively.

Chemical Synthesis. Melting points were determined on a Hoover melting point apparatus and are uncorrected. Infrared (IR) spectra were determined in KBr on a Mattson Cygnus 100 FTIR instrument. Proton magnetic resonance (NMR) were recorded on a Varian Unity 400 MHz spectrometer; shifts are reported in δ units relative to internal tetramethylsilane. Elemental analyses were performed on a CEC Model 240 elemental analyzer, and all compounds submitted for testing had analytical results ±0.4% of the theoretical values. Solutions were dried over anhydrous magnesium sulfate. Column chromatography was accomplished using E. Merck silica gel, 230−400 mesh, and all concentrations were performed in vacuo at 10−30 mmHg.

Preparation of Starting Materials. 2-[(2-Methoxyethoxy)methoxy]benzoic Acid (3). A solution of 15.2 g (100 mmol) of methyl salicylate in 60 mL of THF was cooled to 5 °C and treated portionwise with 4.0 g (100 mmol) of 60% NaH. When addition was complete, the suspension was stirred for 1 h at 5 °C. Neat MEM chloride (15 mL, 130 mmol) was added dropwise, and the reaction mixture was stirred at room temperature for 2 h. Water and EtOAc were added; the organic layer was separated, washed with 1 N NaOH and H_2O, and dried. Concentration gave an oil which was chromatographed on silica gel, eluting with 5:1 hexane:EtOAc. The product so obtained was dissolved in 50 mL of MeOH, treated with 50 mL of 5 M NaOH, and stirred at room temperature for 18 h. The solution was concentrated and the residue dissolved in H_2O. The aqueous solution was washed with Et_2O, acidified to pH 2.5 with 6 N HCl, and extracted with Et_2O. The organic extract was washed with H_2O, dried, and concentrated to give 16.1 g (54%) of the title compound. ^1H NMR ($CDCl_3$): δ 3.37 (s, 3 H), 3.58 (m, 2 H), 3.90 (m, 2 H), 5.50 (s, 2 H), 7.15 (t, 1 H), 7.29 (d, 1 H), 7.53 (m, 1 H), 8.12 (dd, 1 H).

Preparation of Starting Materials. Ethyl 2-[(2-Methoxyethoxy)methoxy]-β-oxobenzenepropanoate (4). A solution of 14.6 g (64.5 mmol) of **3** in 100 mL of dry THF was treated with 12.5 g (77 mmol) of 1,1′-carbonyldiimidazole and stirred at room temperature for 6 h. Meanwhile, a suspension of 6.14 g (64.5 mmol) of anhydrous $MgCl_2$, 15.0 g (88 mmol) of potassium ethyl malonate, and 150 mL of THF was stirred at 50 °C for 6 h and then cooled to room temperature. The solution of crude imidazolide was added to the solution of magnesium malonate, and the reaction mixture was stirred at room temperature for 18 h. The solution was concentrated; the residue was partitioned between $CHCl_3$ and H_2O. The organic layer was separated, washed with 10% aqueous $KHSO_4$ and H_2O, and dried. Concentration gave an oil which was chromatographed on silica gel, eluting with 2:1 hexane:ethyl acetate, to give 15.7 g (82%) of the title compound. ^1H NMR ($CDCl_3$): δ 1.23 (t, 3 H), 3.38 (s, 3 H), 3.56 (m, 2 H), 3.84 (m, 2 H), 3.99 (s, 2 H), 4.18 (q, 2 H), 5.36 (s, 2 H), 7.07 (t, 1 H), 7.27 (d, 1 H), 7.48 (m, 1 H), 7.84 (dd, 1 H).

Preparation of Alkylating Agents: General Procedure A. Synthesis of 1-(3-Bromopropoxy)-3-nitrobenzene (5e). A solution of 13.9 g (100 mmol) of *m*-nitrophenol, 30.2 g (150 mmol) of 1,3-dibromopropane, and 200 mL of THF was treated portionwise with 60% NaH (4.4 g, 110 mmol) and the refluxed for 36 h. The solution was cooled and diluted with H_2O and Et_2O. The organic layer was separated, washed with 5% NaOH and brine, and dried. Concentration gave an oil which was distilled, bp 155−157 °C (5 mmHg), to give the title compound in 26% yield. ^1H NMR ($CDCl_3$): δ 2.37 (m, 2 H), 3.62 (t, 2 H), 4.20 (t, 2 H), 7.25 (m, 1 H), 7.44 (t, 1 H), 7.75 (m, 1 H), 7.85 (dd, 1 H).

5c was prepared in identical fashion from ethyl 3-hydroxybenzoate and 1,3-dibromopropane in 57% yield; similarly, compound **5f** was prepared from 3-methoxyphenol and 1,3-dibromopropane in 48% yield. Compound **5d** was prepared by a similar method from 3-cyanophenol, except that the final product was purified via column chromatography (eluting with EtOAc:hexane, 1:5) to give a 62% yield of the desired product.

Preparation of Alkylating Agents: General Procedure B. Synthesis of [(2-Iodoethoxy)methyl]benzene (5k). A solution of 10.0 g (66 mmol) of 2-(benzyloxy)ethanol in 50 mL of CH_2Cl_2 was cooled to 5 °C and treated with 11.0 mL (78 mmol) of Et_3N and 6.0 mL (77 mmol) of methanesulfonyl chloride, in that order. The mixture was stirred at 5 °C for 1 h and at room temperature for 90 min. Water was added, and the organic layer was washed with saturated $NaHCO_3$ and brine. The solution was dried and concentrated. The residue was dissolved in 100 mL of acetone, treated with 30.0 g (200 mmol) of NaI, and refluxed for 18 h. The suspension was concentrated; the residue was partitioned between Et_2O and H_2O. The organic phase was washed well with H_2O, dried, and concentrated. The product was chromatographed on silica gel, eluting with 5:1 hexane:EtOAc, to give 8.5 g (49%) of the title compound as a red liquid. ^1H NMR ($CDCl_3$): δ 3.28 (t, 2 H), 3.74 (t, 2 H), 4.58 (s, 2 H), 7.29−7.36 (m, 5 H).

Following this procedure, **5l** was prepared in 80% yield from 3-(benzyloxy)propanol. ^1H NMR ($CDCl_3$): δ 2.09 (m, 2 H), 3.31 (t, 2 H), 3.54 (d, 2 H), 4.52 (s, 2 H), 7.34 (m, 5 H).

Preparation of Alkylating Agents: General Procedure C. Synthesis of (3-Iodopropoxy)cyclohexane (5m). A suspension of 9.95 g (60.0 mmol) of 3-phenoxypropionic acid, 0.5 g of PtO_2, and 100 mL of HOAc was shaken in a hydrogen atmosphere of 50 psi at 24 °C for 23 h. The catalyst was filtered, and the filtrate was concentrated to give 9.2 g (89%) of 3-(cyclohexyloxy)propionic acid as a cloudy oil. ^1H NMR ($CDCl_3$): δ 1.18−1.34 (m, 5 H), 1.54 (m, 1 H), 1.73 (m, 2 H), 1.89 (m, 2 H), 2.63 (t, 2 H), 3.31 (m, 1 H), 3.75 (t, 2 H).

To a solution of 9.2 g (53 mmol) of 3-(cyclohexyloxy)propionic acid in 100 mL of dry THF at 5 °C was added 3.8 g (100 mmol) of lithium aluminum hydride portionwise. The mixture was stirred for 48 h at room temperature and then treated with 3.0 mL of H_2O, 4.0 mL of 20% NaOH, and 14 mL of H_2O, in that order. The solids that formed were filtered and washed with Et_2O. The combined filtrate and washings were concentrated to give 6.8 g (81%) of 3-(cyclohexyloxy)propanol as a clear oil. ^1H NMR ($CDCl_3$): δ 1.26 (m, 5 H), 1.53 (m, 1 H), 1.72 (m, 2 H), 1.79−1.91 (m, 5 H), 3.27 (m, 1 H), 3.66 (t, 2 H), 3.78 (t, 2 H).

A solution of crude 3-(cyclohexyloxy)propanol (6.8 g, 43 mmol), 8.2 mL (59 mmol) of Et_3N, and 100 mL of CH_2Cl_2 was cooled to 5 °C and treated with 4.6 mL (59 mmol) of methanesulfonyl chloride. The reaction mixture was stirred at 5 °C for 45 min and at room temperature for 2 h. Water was added, and the organic phase was separated, washed with saturated $NaHCO_3$ and brine, and dried. Concentration gave an oil which was dissolved in 100 mL of acetone and treated with 32.2 g (215 mmol) of NaI. The mixture was refluxed for 20 h, cooled, and concentrated. The residue was partitioned between Et_2O and H_2O; the organic layer was washed well with H_2O, dried, and concentrated. The residue was chromatographed on silica gel, eluting with 5:1 hexane:EtOAc, to give 7.3 g (63%) of the title compound as a red oil. ^1H NMR ($CDCl_3$): δ 1.26 (m, 5 H), 1.54 (m, 1 H), 1.74 (m, 2 H), 1.90 (m, 2 H), 2.03 (m, 2 H), 3.21 (m, 1 H), 3.30 (m, 2 H), 3.51 (t, 2 H).

General Procedure D. Preparation of 3-[3-(3-Chlorophenoxy)propyl]-4-hydroxy-2*H*-1-benzopyran-2-one (28). To a solution of NaOEt in EtOH (0.048 g of sodium in 5 mL of anhydrous EtOH) was added a solution of 0.59 g (2.0 mmol) of ketoester **4**. The mixture was stirred at room temperature for 1 h and then treated with 0.62 g (2.5 mmol) of **5b** and 0.37 g (2.5 mmol) of NaI. The suspension was refluxed for 18 h, cooled to room temperature, and concen-

trated. The residue was partitioned between Et_2O and H_2O; the organic layer was dried and concentrated. The crude product was chromatographed over silica gel (E. Merck, 230–400 mesh), eluting with 2:1 hexane:EtOAc, to give 0.66 g of oil. This material was dissolved in 30 mL of CH_2Cl_2, treated with 1 mL of trifluoroacetic acid, and stirred for 12 h. Concentration gave a residue which was triturated with 1:1 hexane:Et_2O. The solids was filtered, washed with hexane, and dried to give 0.22 g (35% overall yield) of the title compound, mp 169–171 °C. ^{1}H NMR (DMSO-d_6): δ 1.91 (m, 2 H), 2.67 (t, 2 H), 4.02 (t, 2 H), 6.87 (m, 2 H), 6.96 (m, 2 H), 7.28 (m, 2 H), 7.36 (d, 1 H), 7.60 (t, 1 H), 7.93 (dd, 1 H), 11.37 (bs, 1 H). IR: 1663, 1610 cm^{-1}. Anal. ($C_{18}H_{15}ClO_4$) C, H, Cl.

Compounds **1**, **13–16**, **19**, **25**, and **29** were prepared in identical fashion and purified as noted in Table 2. Compounds **21–23** and **34** were prepared in a fashion similar to **28**, starting with ketoester **4** and the appropriate alkyl halide from Table 1. However, in the process of workup and purification of the alkylation step, the MEM protecting group was inadvertently cleaved. Therefore, after chromatography, the adduct was dissolved in 30 mL of CH_2Cl_2, treated with 1 mL of methanesulfonic acid, and refluxed for 2 h. The mixture was cooled and concentrated. For **22** and **34**, the final products were chromatographed on silica gel, eluting with 9:1 $CHCl_3$:MeOH. Compounds **21** and **23** were purified as before by trituration with 1:1 hexane:Et_2O.

General Procedure E. Preparation of 4-Hydroxy-3-[4-(2-methoxyphenyl)butyl]-2*H*-1-benzopyran-2-one (18). A solution of 2.91 g (15.0 mmol) of **9c**, 7 mL (19 mmol) of oxalyl chloride, and 40 mL of CH_2Cl_2 was treated with 3 drops of DMF. The reaction mixture was stirred at room temperature for 2 h and concentrated. This crude acid chloride was added dropwise to a solution of 2.43 g (15.0 mmol) of 4-hydroxycoumarin, 10 drops of piperidine, and 40 mL of pyridine. The resulting mixture was refluxed for 18 h and then cooled to room temperature and poured into ice H_2O. The suspension was acidified to pH 2 with 6 N HCl. The solids obtained were filtered, washed with H_2O, and dried. Recrystallization from EtOH gave 2.7 g of the acyl compound. ^{1}H NMR ($CDCl_3$): δ 2.02 (m, 2 H), 2.74 (t, 2 H), 3.25 (t, 2 H), 3.81 (s, 3 H), 6.82–6.90 (m, 2 H), 7.16 (m, 2 H), 7.26–7.52 (m, 2 H), 7.69 (t, 1 H), 8.06 (d, 1 H).

A solution of 1.02 g (3.01 mmol) of the product obtained above in 10 mL of HOAc was heated to 100 °C and treated portionwise with 0.40 g (6.4 mmol) of sodium cyanoborohydride. The mixture was stirred at room temperature for 1 h. H_2O (20 mL) was added, and the solids were filtered and washed with H_2O. Recrystallization from EtOH:H_2O gave 0.75 g (40% overall yield) of the title compound, mp 123–124 °C. ^{1}H NMR (DMSO-d_6): δ 1.63 (m, 4 H), 2.64 (t, 4 H), 3.80 (s, 3 H), 6.85 (t, 2 H), 7.13 (d, 2 H), 7.27 (d, 2 H), 7.48 (t, 1 H), 7.92 (d, 1 H).

Compounds **12**, **17**, and **20** were prepared in identical fashion from 4-hydroxycoumarin and the appropriate acid chloride from Table 1. Compounds **31** (prepared from 4,7-dihydroxy-2*H*-1-benzopyran-2-one[37]), **32** (prepared from 4-hydroxy-7-(phenylmethoxy)-2*H*-1-benzopyran-2-one[38]), and **33** (prepared from 4-hydroxy-7-methoxy-2*H*-1-benzopyran-2-one[39]) were synthesized in a similar fashion and purified as noted in Tables 2 and 3.

3-[3-(4-Hydroxy-2-oxo-2*H*-1-benzopyran-3-yl)propoxy]-benzoic Acid (26). A suspension of 0.37 g (1.0 mmol) of compound **25** in 10 mL of EtOH was treated with 1 mL of 20% NaOH and stirred at room temperature for 18 h. The solution was concentrated, and the residue was dissolved in H_2O and washed with Et_2O. The aqueous phase was acidified to pH 4 with 6 N HCl and filtered. The solids were washed with H_2O and dried to give 0.29 g (85%) of the title compound, mp 242–244 °C. ^{1}H NMR (DMSO-d_6): δ 1.93 (m, 2 H), 2.69 (t, 2 H), 4.05 (t, 2 H), 7.16 (m, 1 H), 7.32–7.42 (m, 4 H), 7.54 (m, 1 H), 7.58 (m, 1 H), 7.93 (dd, 1 H), 11.50 (bs, 1 H), 12.97 (bs, 1 H).

4-Hydroxy-3-[3-[3-(hydroxymethyl)phenoxy]propyl]-2*H*-1-benzopyran-2-one (27). A solution of 0.48 g (1.3 mmol) of compound **25** in 40 mL of dry THF was cooled in an ice bath and treated with 1.0 g (26 mmol) of lithium aluminum hydride. The suspension was stirred at 5 °C for 30 min and at room temperature for 3 h. To the mixture were added 0.8 mL of H_2O, 1.0 mL of 20% NaOH, and 3.6 mL of H_2O, in that order. The mixture was stirred for 30 min and filtered, and the filtrate was concentrated. The residue was chromatographed on silica gel (E. Merck, 240–400 ASTM), eluting with 9:1 $CHCl_3$:MeOH, to give 0.19 g (47%) of the title compound, mp 119–121 °C. ^{1}H NMR (DMSO-d_6): δ 1.91 (m, 2 H), 2.68 (t, 2 H), 3.99 (t, 2 H), 4.45 (s, 2 H), 5.15 (bs, 1 H), 6.76 (d, 1 H), 6.86 (m, 2 H), 7.20 (t, 1 H), 7.35 (m, 2 H), 7.59 (m, 1 H), 7.94 (dd, 1 H).

3-[3-(3-Aminophenoxy)propyl]-4-hydroxy-2*H*-1-benzopyran-2-one (24). Compound **23** (0.34 g, 1.0 mmol) was suspended in EtOH (10 mL) and H_2O (10 mL) and treated with 0.17 g (3.0 mmol) of iron filings. The suspension was heated to reflux, and 0.2 mL of 1 N HCl was added slowly. The reaction mixture was refluxed for 3 h and then filtered while hot. The filtrate was concentrated. The residue was chromatographed on silica gel, eluting with 9:1 $CHCl_3$:MeOH, to give 0.14 g (45%) of the title compound, mp 161–162 °C. ^{1}H NMR (DMSO-d_6): δ 1.87 (m, 2 H), 2.65 (t, 2 H), 3.88 (t, 2 H), 6.05 (dd, 1 H), 6.12 (m, 2 H), 6.87 (m, 1 H), 7.35 (m, 2 H), 7.59 (t, 1 H), 7.94 (dd, 1 H).

3-[3-(4-Hydroxy-2-oxo-2*H*-1-benzopyran-3-yl)propoxy]-benzamide (30). A solution of 0.27 g (0.84 mmol) of compound **29** was dissolved in 25 mL of dry *t*-BuOH and treated with 0.24 g (4.2 mmol) of KOH. The mixture was refluxed for 2 h, cooled to room temperature, and concentrated. The residue was dissolved in H_2O, washed with Et_2O, and acidified to pH 2 with 6 M HCl. The solids which precipitated were filtered, washed with EtOH–Et_2O, and dried in vacuo to give the title compound, mp 197–198 °C. ^{1}H NMR (DMSO-d_6): δ 1.93 (m, 2 H), 2.70 (t, 2 H), 4.05 (t, 2 H), 7.06 (m, 1 H), 7.28–7.47 (m, 4 H), 7.60 (t, 1 H), 7.96 (m, 2 H).

4-Hydroxy-3-(3-hydroxypropyl)-2*H*-1-benzopyran-2-one (35). A mixture of 0.12 g (0.4 mmol) of **21**, 0.05 g of palladium on carbon, and 75 mL of MeOH was shaken in a hydrogen atmosphere (52 psi) at room temperature for 20 min. The catalyst was filtered, and the filtrate was concentrated. The residue was triturated with Et_2O, and the solids were filtered to give 0.08 g (95%) of the title compound, mp 109–110 °C. ^{1}H NMR (DMSO-d_6): δ 1.62 (m, 2 H), 2.54 (m, 2 H), 3.44 (t, J = 6.7 Hz, 2 H), 7.35 (m, 2 H), 7.59 (m, 1 H), 7.91 (dd, 1 H), 11.28 (bs, 1 H).

4-Hydroxy-3-[3-(hydroxyimino)-3-phenylpropyl]-2*H*-1-benzopyran-2-one (37). To a solution of $NaOCH_3$ (0.087 mmol) in MeOH (10 mL) was added 0.060 g (0.86 mmol) of hydroxylamine hydrochloride. When addition was complete, 0.21 g (0.71 mmol) of **36**[40] was added portionwise and the mixture was stirred for 18 h at room temperature. The solvent was evaporated, and the residue was partitioned between $CHCl_3$ and H_2O. The organic layer was dried and concentrated. The product was recrystallized from EtOAc:hexane to give 0.17 g (75%) of the title compound. ^{1}H NMR (DMSO-d_6): δ 2.70–2.78 (m, 2 H), 2.93 (m, 2 H), 7.35 (m, 5 H), 7.58 (m, 1 H), 7.74 (m, 2 H), 7.96 (d, 1 H).

4-Hydroxy-3-[(2-phenoxyethyl)thio]-2*H*-1-benzopyran-2-one (38). A solution of 0.65 g (4.0 mmol) of 4-hydroxycoumarin in EtOH (30 mL) was treated with a solution of 0.16 g (4.0 mmol) of NaOH in H_2O (10 mL) and then with 1.24 g (4.0 mmol) of 2-phenoxyethyl *p*-toluenethiolsulfonate.[41] The mixture was refluxed for 18 h, cooled to room temperature, and concentrated. The residue was partitioned between $CHCl_3$ and H_2O. The organic layer was dried and concentrated. The product was chromatographed on silica gel, eluting with 10:1 hexane:EtOAc, to give 0.85 g (67%) of the title compound, mp 120–121 °C. ^{1}H NMR ($CDCl_3$): δ 3.21 (t, 2 H), 4.11 (t, 2 H), 6.86 (d, 2 H), 6.97 (t, 1 H), 7.25–7.37 (m, 4 H), 7.62 (d, 1 H), 7.88 (d, 1 H), 8.39 (bs, 1 H).

4-Hydroxy-3-(3-phenoxypropyl)-2(1*H*)-quinolinone (39). A solution of 3.1 g (11 mmol) of (3-phenoxypropyl)diethyl propanedioate[44] in 11 mL of diphenyl ether was heated to reflux and treated with 1.1 g (12 mmol) of aniline via syringe pump over 4 H. After addition was complete, the reaction mixture was refluxed for 4 h. The solution was cooled, and the diphenyl ether was removed by vacuum distillation. The remaining solid was a mixture of **39** and *N*,*N*'-diphenyl(3-

phenoxypropyl)propanedicarboxamide. This mixture was triturated with ether, and the ether filtrate was concentrated to afford 0.14 g (4%) of the title compound, mp 170–171 °C. ^{1}H NMR (DMSO-d_6): δ 1.90 (t, 2 H), 2.71 (t, 2 H), 3.99 (t, 2 H), 6.90 (m, 3 H), 7.14 (m, 1 H), 7.27 (m, 3 H), 7.44 (m, 1 H), 7.90 (d, 1 H), 10.18 (s, 1 H), 11.32 (s, 1 H).

References

(1) Tomasselli, A. G.; Howe, J. W.; Sawyer, T. K.; Wlodawer, A.; Heinrikson, R. L. The complexities of AIDS: An assessment of the HIV protease as a therapeutic target. *Chim. Oggi* **1991**, *9*, 6–27.

(2) Martin, J. A. Recent advances in the design of HIV proteinase inhibitors. *Antiviral Res.* **1992**, *17*, 265–278.

(3) Kohl, N. E.; Emini, E. A.; Schleif, W. A.; Davis, L. I.; Heimbach, J. C.; Dixon, R. A.; Scolnick, E. M.; Sigal, I. S. Active human immunodeficiency virus protease is required for viral infectivity. *Proc. Natl. Acad. Sci. U.S.A.* **1988**, *85*, 4686–4690.

(4) McQuade, T. K.; Tomasselli, A. G.; Liu, L.; Karacostas, V.; Moss, B.; Sawyer, T. K.; Heinrikson, R. L.; Tarpley, W. G. Synthetic HIV-1 protease inhibitor with antiviral activity arrests HIV-like particle maturation. *Science* **1990**, *247*, 454–456.

(5) Seelmeier, S.; Schmidt, H.; Turk, V.; von der Helm, K. Human immunodeficiency virus has an aspartic-type protease that can be inhibited by pepstatin A. *Proc. Natl. Acad. Sci. U.S.A.* **1988**, *85*, 6612–6616.

(6) Kaplan, A. H.; Zack, J. A.; Knigge, M.; Paul, D. A.; Kempf, D. J.; Norbeck, D. W.; Swanstrom, R. J. Partial inhibition of the human immunodeficiency virus type 1 protease results in aberrant virus assembly and the formation of noninfectious particles. *J. Virol.* **1993**, *67*, 4050–4055.

(7) Toh, H.; Ono, M.; Saigo, K.; Miyata, T. Retroviral protease-like sequence in the yeast transposon Ty1. *Nature* **1985**, *315*, 691–692.

(8) Miller, M.; Jaskolski, M.; Rao, J. K. M.; Leis, J.; Wlodawer, A. Crystal structure of a retroviral protease proves relationship to aspartic protease family. *Nature* **1989**, *337*, 576–579.

(9) Wlodawer, A.; Erickson, J. W. Structure based inhibitors of HIV-1 protease. *Annu. Rev. Biochem.* **1993**, *62*, 543–585.

(10) Appelt, K. Crystal structures of HIV-1 protease-inhibitor complexes. *Perspect. Drug Discovery Des.* **1993**, *1*, 23–48.

(11) Graves, B. J.; Hatada, M. H.; Miller, J. K.; Graves, M. C.; Roy, S.; Cook, C. M.; Krohn, A.; Martin, J. A.; Roberts, N. A. The three-dimensional X-ray crystal structure of HIV-1 protease complexed with a hydroxyethylene inhibitor. In *Structure and Function of the Aspartic Proteinases*; Dunn, B., Ed.; Plenum Press: New York, 1992; pp 455–460.

(12) Thompson, W. J.; Fitzgerald, P. M. D.; Holloway, M. K.; Emini, E. A.; Darke, P. L.; McKeever, B. M.; Schleif, W. A.; Quintero, J. C.; Zugay, J. A.; Tucker, T. J.; Schwering, J. E.; Homnick, C. F.; Nunberg, J.; Springer, J. P.; Huff, J. R. Synthetic and antiviral activity of a series of HIV-1 protease inhibitors with functionality tethered to the P1 or P1′ phenyl substituents: X-ray crystal structure assisted design. *J. Med. Chem.* **1992**, *35*, 1685–1701.

(13) The 'P' subsite nomenclature relates amino acid residues or mimics in the inhibitor to corresponding residues in the natural substrate. The 'S' nomenclature relates in terms of the enzyme subsites. Schechter, I.; Berger, A. On the size of the active site in proteases I. Papain. *Biochem. Biophys. Res. Commun.* **1967**, *27*, 157–162.

(14) Clare, M. HIV protease: Structure-based design. *Perspect. Drug Discovery Des.* **1993**, *1*, 49–68.

(15) Wlodawer, A.; Miller, M.; Jaskolski, M.; Sathyanarayana, B. K.; Baldwin, E.; Weber, I. T.; Selk, L. M.; Clawson, L.; Schneider, J.; Kent, S. B. H. Conserved folding in retroviral proteases: Crystal structure of a synthetic HIV-1 protease. *Science* **1989**, *245*, 616–621.

(16) Erickson, J. W. Design and structure of symmetry-based inhibitors of HIV-1 protease. *Perspect. Drug Discovery Des.* **1993**, *1*, 109–128.

(17) Verhoef, J. C.; Bodde, H. E.; de Boer, A. G.; Bouwstra, J. A.; Junginger, H. E.; Merkus, F. W.; Breimer, D. D. Transport of peptide and protein drugs across biological membranes. *Eur. J. Drug Metab. Pharmacokinet.* **1990**, *15*, 83–93.

(18) Kuntz, I. D.; Blaney, J. M.; Oatley, S. J.; Langridge, R.; Ferrin, T. E. A geometric approach to macromolecular-ligand interactions. *J. Mol. Biol.* **1982**, *161*, 269–288.

(19) DesJarlais, R. L.; Seibel, G. L.; Kuntz, I. D.; Furth, P. S.; Alvarez, J. C.; Ortiz de Montellano, P. R.; DeCamp, D. L.; Babe, L. M.; Craik, C. S. Structure based design of nonpeptide inhibitors specific for the human immunodeficiency virus. *Proc. Natl. Acad. Sci. U.S.A.* **1990**, *87*, 6644–6648.

(20) Lam, P. Y. S.; Jadhav, P. K.; Eyermann, C. J.; Hodge, C. N.; Ru, Y.; Bacheler, L. T.; Meek, J. L.; Otto, M. J.; Rayner, M. M.; Wong, Y. N.; Chang, C.-H.; Weber, P. C.; Jackson, D. A.; Sharpe, T. R.; Erickson-Viitanen, S. K. Rational design of potent bioavailable nonpeptide cyclic ureas as HIV protease inhibitors. *Science* **1994**, *264*, 380–383.

(21) Appelt, K. 33rd Interscience Conference on Antimicrobial Agents & Chemotherapy, New Orleans, LA, 1993.

(22) Humber, D. C.; Cammack, N.; Coates, J. A. V.; Cobley, K. N.; Orr, D. C.; Weingarten, G. G.; Weir, M. P. Penicillin derived C_2-symmetric dimers as novel inhibitors of HIV-1 proteinase *J. Med. Chem.* **1992**, *35*, 3080–3081.

(23) Ondeyka, J.; Hensens, O. D.; Zink, D.; Ball, R.; Lingham, R. B.; Bills, G.; Dombrowski, A.; Goetz, M. L-696,474, a novel cytochalasin as an inhibitor of HIV-1 protease. II. Isolation and structure. *J. Antibiot.* **1992**, *45*, 679–685.

(24) Tummino, P. J.; Ferguson, D.; Hupe, L.; Hupe, D. Competitive inhibition of HIV-1 protease by 4-hydroxy-benzopyran-2-ones and by 4-hydroxy-6-phenylpyran-2-ones. *Biochem. Biophys. Res. Commun.* **1994**, *200*, 1658–1664.

(25) Ukita, T.; Nojima, S.; Matsumoto, M. Synthesis of 3-alkylated or 3-acetylated 4-hydroxycoumarins and of a related pyrone. *J. Am. Chem. Soc.* **1950**, *72*, 5143–5144.

(26) Nutaitis, C. F.; Schultz, R. A.; Obaza, J.; Smith, F. X. Reduction of isopropylidene acylmalonates, 5-acylbarbituric acids, and 3-acyl-4-hydroxycoumarins to the corresponding alkyl derivatives by sodium cyanoborohydride-acetic acid. *J. Org. Chem.* **1980**, *45*, 4606–4608.

(27) Blundell, T. L.; Jenkins, J. A.; Sewell, B. T.; Pearl, L. H.; Cooper, J. B.; Wood, S. P.; Veerapandian, B. X-ray analyses of aspartic proteinases. The three dimensional structure at 2.1 Å resolution of endothiapepsin. *J. Mol. Biol.* **1990**, *211*, 919–941.

(28) Suguna, K.; Padian, E. A.; Smith, C. W.; Carlson, W. D.; Davies, D. R. Binding of a reduced peptide inhibitor to the aspartic proteinase from *Rhizopus chinensis*: Implications for a mechanism of action. *Proc. Natl. Acad. Sci. U.S.A.* **1987**, *84*, 7009–7013.

(29) Rutenber, E.; Fauman, E. B.; Keenan, R. J.; Fong, S.; Furth, P. S.; Oritz deMontellano, P. R.; Meng, E.; Kuntz, I. D.; DeCamp, D. L.; Salto, R.; Rose, J. R.; Craik, C. S.; Stroud, R. M. Structure of a non-peptide inhibitor complexed with HIV-1 protease. Developing a cycle of structure-based drug design. *J. Biol. Chem.* **1993**, *268*, 15343–15346.

(30) Miller, M.; Schneider, J.; Sathyanarayana, B. K.; Toth, M. V.; Marshall, G. R.; Clawson, L.; Selk, L.; Kent, S. B. H.; Wlodawer, A. Structure of a complex of synthetic HIV-1 protease with a substrate-based inhibitor at 2.3 Å resolution. *Science* **1989**, *246*, 1149–1152.

(31) Goodsell, D. S.; Olson, A. J. Automated docking of substrates to proteins by simulated annealing. *Proteins: Struct., Funct., Genet.* **1990**, *8*, 195–202.

(32) Bhat, T. N.; Erickson, J. W. Unpublished results.

(33) (a) Goodford, P. J. A computational procedure for determining energetically favorable binding sites in biologically important macromolecules. *J. Med. Chem.* **1985**, *28*, 849–857. (b) GRID Software Program, Molecular Discovery Ltd., West Way House, Elms Parade, Oxford OX2 9LL, England.

(34) Vara Prasad, J. V. N.; Para, K. S.; Lunney, E. A.; Ortwine, D. F.; Dunbar, J. B.; Ferguson, D.; Tummino, P. J.; Hupe, D.; Tait, B. D.; Domagala, J. M.; Humblet, C.; Bhat, T. N.; Liu, B.; Guerin, D. M. A.; Baldwin, E. T.; Erickson, J. W.; Sawyer, T. K. Novel series of achiral, low molecular weight and potent HIV-1 protease inhibitors. *J. Am. Chem. Soc.* **1994**, in press.

(35) Jordan, S. P.; Zugay, J.; Darke, P. L.; Kuo, L. C. Activity and dimerization of human immunodeficiency virus protease as a function of solvent composition and enzyme concentration. *J. Biol. Chem.* **1992**, *267*, 20028–20032.

(36) (a) Sybyl Molecular Modeling Software, Versions 5 and 6, Tripos Associates Inc., 1699 S. Hanley Rd., Suite 303, St. Louis, MO 63144. (b) Clark, M.; Cramer, R. D., III; Van Opdenbosch, N. Validation of the general purpose tripos 5.2 force field. *J. Comput. Chem.* **1989**, *10*, 982–1012.

(37) Pandey, G.; Muralikrishna, C.; Bhalerao, U. T. Mushroom tyrosinase-catalyzed synthesis of coumestans, benzofuran derivatives, and related heterocyclic compounds. *Tetrahedron* **1989**, *45*, 6867–6874.

(38) Hermodson, M. A.; Barker, W. M.; Link, K. P. Studies on the 4-hydroxycoumarins. Synthesis of the metabolites and some other derivatives of warfarin. *J. Med. Chem.* **1971**, *14*, 167–169.

(39) Knierzinger, A.; Wolfbeis, O. S. Synthesis of fluorescent dyes. IX. New 4-hydroxycoumarins, 4-hydroxy-2-quinolones, 2H,5H-pyrano[3,2-c]benzopyran-2,5-diones and 2H,5H-pyrano[3,2-c]-quinoline-2,5-diones. *J. Heterocycl. Chem.* **1980**, *17*, 225–229.

(40) Bravo, P.; Ticozzi, C. Alkylation of 4-hydroxycoumarins by ketone Mannich bases. Synthesis of 4-hydroxy-2-oxo-3-(3-oxoalkyl)-2H-1-benzopyrans. *Synthesis* **1985**, 894–896.

(41) Dunbar, J. E. U.S. Patent 3 810 922, 1974; *Chem. Abstr. 81*, 49568c.

(42) Pattison, I. C. U.S. Patent 4 292 321, 1981; *Chem. Abstr. 96*, 6732u.

(43) Sanchez, I. H.; Aguilar, M. A. Synthesis of 4-arylbutanenitriles. *Synthesis* **1981**, *1*, 55–56.

(44) Gunther, A. Synthese des *d*- and *l*-β-aethyl piperidins. (Synthesis of the *d* and *l*-β-ethyl piperidines.) *Chem. Ber.* **1898**, *31*, 2134–2142.